Spring 2019

Modelling Potential Fluctuations in Double Layer Graphene Systems as a Periodic Oscillation in Electron Density & its Effect on Coulomb Drag

Ryan Bogucki
rab175@zips.uakron.edu

MODELLING POTENTIAL FLUCTUATIONS IN DOUBLE LAYER GRAPHENE SYSTEMS AS A PERIODIC OSCILLATION IN ELECTRON DENSITY & ITS EFFECT ON COULOMB DRAG

An Honors Project

Presented to

The Faculty of The University of Akron

In Partial Fulfillment

of the Requirements for the Degree

Honors Bachelor of Physics

Ryan Anthony Bogucki

May, 2019

ABSTRACT

An expression for the drag transresistivity in a graphene double layer system exhibiting potential fluctuations modelled as a periodic oscillation in electron density is derived. Our model starts from the Coulombic interaction and we derive the correlation between a sinusoidal fluctuation in electron density in the first layer and the induced electron density in the second layer. Previous models in the literature have employed an arbitrary correlation between each layer's electron density, and the model presented is the first attempt in the literature to explicitly derive this correlation. Recent experiments have found that the drag transresistivity in graphene double layers systems exhibit a sign change as the electron density in the first layer is increased from zero. Our model is able to reproduce this sign change, and is in agreement with experiment. As the amplitude of the fluctuations approaches zero, the model reproduces the result of the uniform case. The model qualitatively agrees with experimental results, but it needs to be further refined to more accurately take into account how electron density fluctuations actually occur in experimental samples.

TABLE OF CONTENTS

LIST OF FIGURES

CHAPTER I

INTRODUCTION

In general, Coulomb drag is a phenomenon in which long range Coulombic interactions between isolated conductors induce a current in one conductor when an electrical current is applied in the other (Figure 1.1). This phenomenon has been widely studied both theoretically and experimentally for two dimensional electron gasses (an electron gas that is free to move in two dimensions, but narrowly restricted in the third). Layered systems of two dimensional electron gasses are of particular interest. The study of graphene has seen a surge of research in recent years, including layered 2d systems of graphene, which can be modelled as a layered system of 2d electron gasses. The curious result of previous experiments on layered 2d graphene sheets have found that as the electron density in either sheet increases form zero, there exists a point where the induced current, and as a result the drag transresistivity ρ_{drag}, reverses sign [2, 3, 4]. The drag transresistivity ρ_{drag}, defined as a ratio of the induced voltage in the non-driven layer to the applied current in the driven layer, is relatively simple to measure, making it the probe of choice for experiments. As such, ρ_{drag} is the clear parameter to build theories on to relate to experiment. The authors theorized that this reversal of sign may be caused by inhomogeneities within the sample, motivating an investigation of the nature these inhomogeneities. Previous

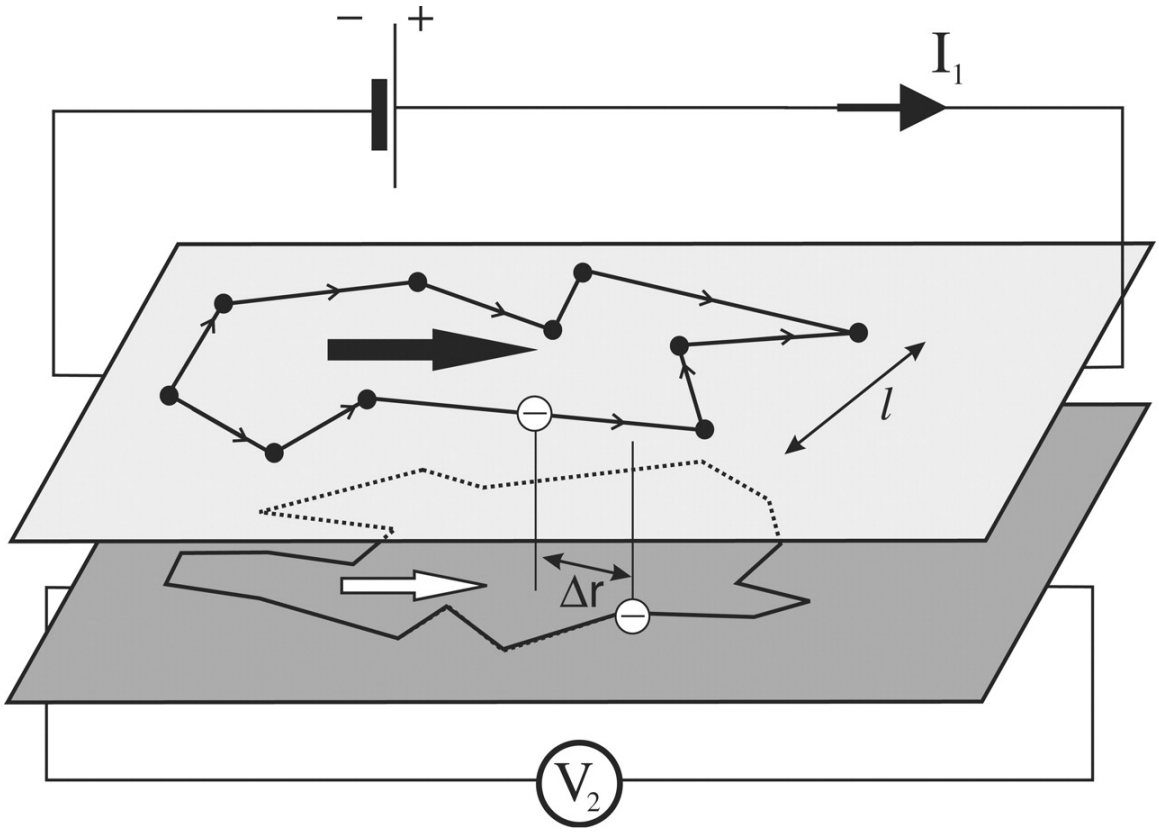

Figure 1.1: The induced voltage V_2 induced by the current in the driven layer, I_1. The ratio of V_2 to I_2 is defined to be ρ_{drag}. From (Narozhny & Levchenko, 2016, p. 2)[1]

theoretical works have confirmed that inhomogeneities in graphene do contribute to the total drag transresistivity [5, 6], but the exact mechanism through which this happens is unclear. The mathematical formulation of these inhomogeneities has not been well studied, and the aim of this work is elucidate the mechanism by which they contribute to the drag transresistivity.

In this work, we develop a theory of Coulomb drag in inhomogeneous 2D graphene modelled as periodic oscillations in the electron density of the driving layer. We start from the simple case where oscillations can be modelled as a sine wave, and

we derive an expression in chapter two that relates the amplitude of oscillation in the driven layer to the external potential that it induces. Previous theoretical models have employed an arbitrary correlation between the fluctuations in electron density to the potential that they induce [6], whereas in our model this correlation is derived from the interlayer Coulomb interactions. Our theory does not apply in the presence of external fields, such as magnetic or other electric fields.

CHAPTER II

MODEL FOR ELECTRON DENSITY OSCILLATION

2.1 External Potential Calculation

First, we model potential fluctuations in graphene as a periodic oscillation in electron density in layer one, with a constant electron density in layer two, as shown in Figure 2.1. Figure 2.2 qualitatively shows how the charge density in the second layer, n_2, shifts due to the charge density fluctuation in the first.

$$n_1(\vec{r}_{2d}) = \overline{n}_1 + \delta n_1 e^{i\vec{q}\cdot\vec{r}_{2\mathrm{d}}} \tag{2.1}$$

Where $\overline{n}_1$ is the uniform charge density, and δn_1 is the amplitude of oscillation. The induced potential in the second plate can then be written as

$$\phi_1(\vec{r}_{2\mathrm{d}}, d) = \frac{1}{4\pi\varepsilon_0}\int \frac{n(\vec{r'})}{|\vec{r'} - \vec{r}_{2\mathrm{d}} - d\hat{z}|}d\vec{r'} = \frac{\delta n_1 e^{i\vec{q}\cdot\vec{r}_{2\mathrm{d}}}}{4\pi\varepsilon_0}\int \frac{e^{i\vec{q}\cdot(\vec{r'}-\vec{r}_{2\mathrm{d}})}}{|\vec{r'} - \vec{r}_{2\mathrm{d}} - d\hat{z}|}d\vec{r'} \tag{2.2}$$

We have omitted $\overline{n_1}$ from equation (2.2), as it only serves to offset the result, and does not contribute in a significant way. Making the substitution $\vec{R} = |\vec{r'} - \vec{r}_{2\mathrm{d}}|$ yields

$$\phi_1(\vec{r}_{2\mathrm{d}}, d) = \frac{\delta n_1 e^{i\vec{q}\cdot\vec{r}_{2d}}}{4\pi\varepsilon_0}\int \frac{e^{i\vec{q}\cdot\vec{R}}}{|\vec{R} - d\hat{z}|}d\vec{R} \tag{2.3}$$

To make progress, the integral above must be taken into polar coordinates (s is the radial component)

$$\phi_1(\vec{r}_{2\mathrm{d}}, d) = \frac{\delta n_1 e^{i\vec{q}\cdot\vec{r}_{2d}}}{4\pi\varepsilon_0}\int_0^{2\pi} d\theta \int_0^{\infty} \frac{s e^{iqscos(\theta)}}{\sqrt{s^2 + d^2}}ds \tag{2.4}$$

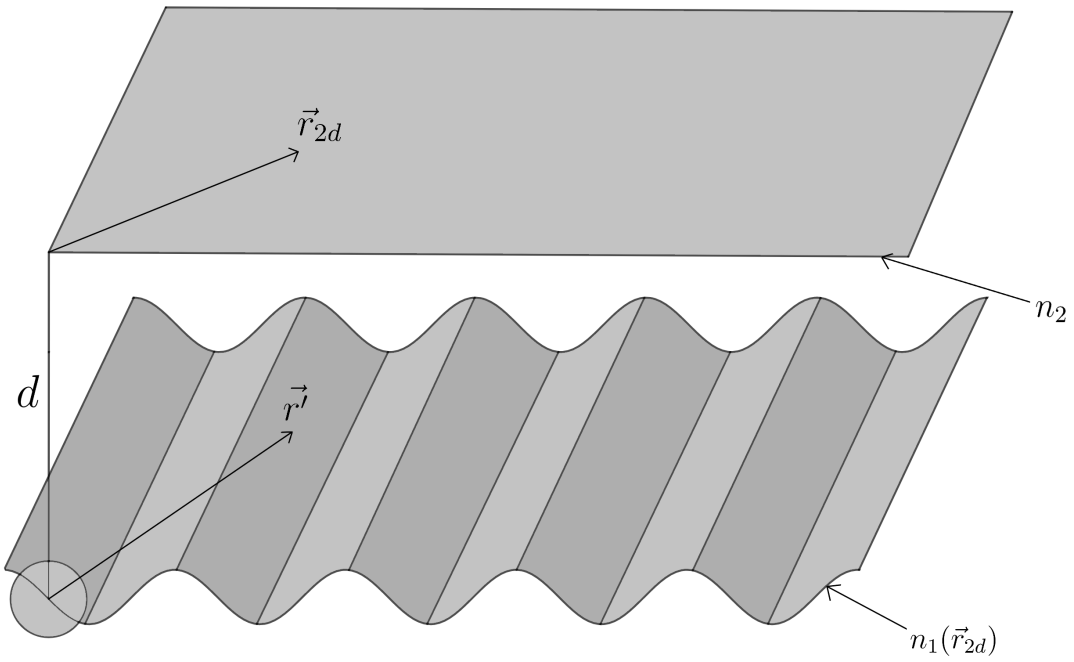

Figure 2.1: Model of oscillating charge density n_1, and initially a constant charge density n_2. The oscillation depicted in the contour above represents a spatial oscillation in electron density in the first layer.

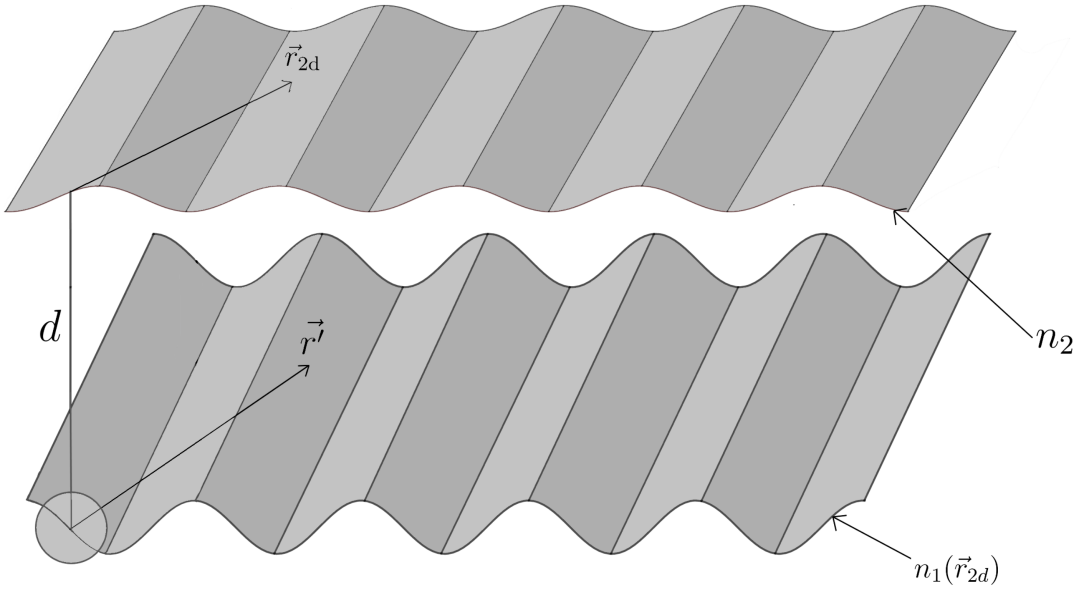

Figure 2.2: Model of oscillating charge density n_1, with a charge density n_2 that has been created due to the electric potential caused by the charge density fluctuation in the first layer. The oscillations depicted in the contour above represent spatial oscillations in electron densities of each layer.

Integrating with respect with θ first yields a Bessel function

$$\phi_1(\vec{r}_{2\mathrm{d}}, d) = \frac{\delta n_1 e^{i\vec{q}\cdot\vec{r}_{2\mathrm{d}}}}{2\varepsilon_0} \int_0^\infty \frac{sJ_0(qs)}{\sqrt{s^2+d^2}} ds \tag{2.5}$$

The result of this integral is $\frac{1}{qe^{qd}}$. The resulting potential is then

$$\phi_1(\vec{r}_{2\mathrm{d}}, d) = \frac{\delta n_1 e^{(i\vec{q}\cdot\vec{r}_{2\mathrm{d}} - qd)}}{2\varepsilon_0 q} \tag{2.6}$$

2.2 External Potential and Induced Charge Density Relation

To relate the change in electron density in the second layer, δn_2, due to the electron density fluctuation in the first, δn_1, we first must introduce another potential: one that is due to the electron density fluctuation δn_2 in layer 2, ϕ_2. Then we also define the total potential

$$\phi_{\mathrm{tot}} = \phi_1 + \phi_2 \tag{2.7}$$

$\phi_2(\vec{r})$ must obey Poisson's equation.

$$-\bigtriangledown^2 \phi_2(\vec{r}) = \frac{\delta n_2}{\varepsilon_0} \tag{2.8}$$

$\phi_{\mathrm{tot}}(\vec{r})$ and $\phi_1(\vec{r})$ are related by the dielectric function $\varepsilon_{\mathrm{r}}(\vec{r}-\vec{r'})$ through the following integral

$$\phi_1(\vec{r}) = \int d\vec{r'} \varepsilon_{\mathrm{r}}(\vec{r}-\vec{r'}) \phi_{\mathrm{tot}}(\vec{r'}) \tag{2.9}$$

The integral above requires a convolution integral making it difficult to work with. To simplifiy the situation, we will take the Fourier transform of the integral, which is given as

$$\phi_1(\vec{q}) = \varepsilon_r(\vec{q}) \phi_{\mathrm{tot}}(\vec{q}) \tag{2.10}$$

We then introduce χ_q which is defined as

$$\delta n_2 = \chi_q \phi_{\text{tot}}(\vec{q}) \tag{2.11}$$

We must also take the Fourier transforms of the Poisson's equations to make progress, and in two dimensions the Poisson equation for the second layer becomes

$$\phi_2(\vec{q}) = \frac{\delta n_2}{2q\varepsilon_0} \tag{2.12}$$

For details about this Fourier transform, see the appendix. Rearraging equation (2.12) and combining with equation (2.7) yields

$$\delta n_2 = 2q\varepsilon_0(\phi_{\text{tot}}(\vec{q}) - \phi_1(\vec{q})) \tag{2.13}$$

And combining with equation (2.11) yields

$$\delta n_2 = 2q\varepsilon_0(\frac{\delta n_2}{\chi_2} - \phi_1(\vec{q})) \tag{2.14}$$

$$\delta n_2 = \phi_1(\vec{q})\frac{\chi_2}{1 - \frac{\chi_2}{2q\varepsilon_0}} \tag{2.15}$$

The final step is to relate δn_2 to δn_1 through the potential created by the first layer found in equation (2.6) which gives

$$\delta n_2 = \delta n_1 \frac{e^{-qd}}{2\varepsilon_0 q}\frac{\chi_2}{1 - \frac{\chi_2}{2q\varepsilon_0}} \tag{2.16}$$

$$= \delta n_1 \frac{\chi_2}{2\varepsilon_0 q - \chi_2} e^{-qd} \tag{2.17}$$

The $e^{i\vec{q}\cdot\vec{r}_{2\text{d}}}$ term from equation (2.6) has been neglected here, as the spatial dependence that $e^{i\vec{q}\cdot\vec{r}_{2\text{d}}}$ brings is already implied within Fourier space.

2.3 Drag Transresistivity Calculation

Now that we have derived an expression relating the induced charge density to the external potential, we will shift our attention towards calculating the drag transresistivity, $\rho_{\text{drag}}(n_1, n_2)$. Because the variation in charge density is periodic, we can average over one period. Therefore, we define the average drag transresistivity over one period, $\overline{\rho}_{drag}$, to be

$$\overline{\rho}_{\text{drag}} = \frac{q}{2\pi}\int_0^{\frac{2\pi}{q}} \rho_{\text{drag}}(n_1 + \delta n_1 \cos(qx), n_2 + \delta n_2 \cos(qx))dx \tag{2.18}$$

Taylor expanding around n_1 and n_2 yields

$$\begin{aligned}\overline{\rho}_{\text{drag}} = \frac{q}{2\pi}\int_0^{\frac{2\pi}{q}} \Big[\rho_{\text{drag}}(n_1, n_2) + \frac{\partial^2 \rho_{\text{drag}}}{\partial n_1 \partial n_2}\cos^2(qx)\delta n_1 \delta n_2 \\ + \frac{1}{2}\frac{\partial^2 \rho_{\text{drag}}}{\partial {n_1}^2}\cos^2(qx)\delta {n_1}^2 + \frac{1}{2}\frac{\partial^2 \rho_{\text{drag}}}{\partial {n_2}^2}\cos^2(qx)\delta {n_2}^2\Big]dx\end{aligned} \tag{2.19}$$

$$\begin{aligned}= \rho_{\text{drag}}(n_1, n_2)\frac{q}{2\pi}\Big(\int_0^{\frac{2\pi}{q}} dx\Big) + \Big[\int_0^{\frac{2\pi}{q}} \cos^2(qx)dx\Big]\Big(\frac{\partial^2 \rho_{\text{drag}}}{\partial n_1 \partial n_2}\delta n_1 \delta n_2 \\ + \frac{1}{2}\frac{\partial^2 \rho_{\text{drag}}}{\partial {n_1}^2}\delta {n_1}^2 + \frac{1}{2}\frac{\partial^2 \rho_{\text{drag}}}{\partial {n_2}^2}\delta {n_2}^2\Big)\end{aligned} \tag{2.20}$$

But now we notice that $\int_0^{\frac{2\pi}{q}} \cos^2(qx)dx = \frac{\pi}{q}$ and $\frac{q}{2\pi}\int_0^{\frac{2\pi}{q}} dx = 1$. Also, δn_1 is related to δn_2 through equation (2.17). Using these results, we simplify equation (2.20) as

$$\overline{\rho}_{\text{drag}} = \rho_{\text{drag}}(n_1, n_2) + \frac{1}{2}(\delta {n_1}^2)\left[\frac{\partial^2 \rho_{\text{drag}}}{\partial n_1 \partial n_2}\frac{\chi_2 e^{-qd}}{2\varepsilon_0 q - \chi_2} + \frac{1}{2}\frac{\partial {\rho_{\text{drag}}}^2}{\partial {n_2}^2}\frac{\chi_2^2 e^{-2qd}}{(2\varepsilon_0 q - \chi_2)^2} + \frac{1}{2}\frac{\partial^2 \rho_{\text{drag}}}{\partial {n_1}^2}\right] \tag{2.21}$$

To simplify even further, we will let

$$\chi_{\text{sep}} \equiv \frac{\chi_2 e^{-qd}}{2\varepsilon_0 q - \chi_2} \tag{2.22}$$

which is dimensionless. This leads to

$$\overline{\rho}_{\text{drag}} = \frac{q}{2\pi}\int_0^{\frac{2\pi}{q}} \rho_{\text{drag}}(n_1, n_2)dx + \frac{1}{2}(\delta {n_1}^2)\left[\frac{\partial^2 \rho_{\text{drag}}}{\partial n_1 \partial n_2}\chi_{\text{sep}} + \frac{1}{2}\frac{\partial^2 \rho_{\text{drag}}}{\partial {n_2}^2}{\chi_{\text{sep}}}^2 + \frac{1}{2}\frac{\partial^2 \rho_{\text{drag}}}{\partial {n_1}^2}\right] \tag{2.23}$$

2.4 Test with model of drag transresistivity

The next step is to see how equation (2.23) performs, given a model of ρ_{drag}. In the case where the interlayer distance, d, is much larger than the average distance between electrons in each layer and the Fermi energy $\varepsilon_{\text{F}} > k_{\text{B}}T$, Tse et. al [7] demonstrates that drag transresistivity at low temperatures is given as

$$\rho_{\text{drag}} = -\frac{h}{e^2}\frac{\pi\zeta(3)}{32}\frac{(k_{\text{B}}T)^2}{\varepsilon_{\text{F1}}\varepsilon_{\text{F2}}}\frac{1}{(q_{\text{TF1}}d)(q_{\text{TF2}}d)}\frac{1}{(k_{\text{F1}}d)(k_{\text{F2}}d)} \tag{2.24}$$

Where $q_{\text{TF}} = 4e^2\frac{k_{\text{F}}}{v}$ is the Thomas-Fermi wave number for extrinsic graphene, $\varepsilon_{\text{F}} = v\hbar k_{\text{F}}$ is the Fermi energy with respect to the dirac point and ζ is the Riemann zeta function [8]. In both ε_{F} and q_{TF}, v is the electron velocity in graphene and $k_{\text{F}} = \sqrt{2\pi n}$ is the Fermi wavevector for each respective sheet. We are interested in an expression that depends on the electron densities in the two sheets so that the expression can be used with equation (2.23). Using the expressions for q_{TF}, ε_{F} and k_{F} we can rewrite equation (2.24) as

$$\rho_{\text{drag}} = -\frac{h\zeta(3)}{e^6 \cdot 1024}\frac{(k_{\text{B}}T)^2}{d^4}\frac{1}{n_1^{3/2}n_2^{3/2}} \tag{2.25}$$

However, this expression, which was derived under the assumption that $\varepsilon_{\text{F}} > k_{\text{B}}T$, leads to unphysical behavior as n_1 or n_2 approach 0. Experimental studies have shown that when n_1 or n_2 approaches zero, ρ_{drag} also approaches zero [2, 4, 3]. To account

for this, we introduce a correction factor $n_0(T)$ such that

$$\frac{1}{n^{3/2}} \rightarrow \frac{n}{(n^{5/2} + n_0^{5/2})} \tag{2.26}$$

With this modification, equation (2.25) becomes

$$\rho_{\text{drag}} = -\frac{h\zeta(3)}{e^6 \cdot 1024} \frac{(k_{\text{B}}T)^2}{d^4} \frac{n_1 n_2}{(n_1^{5/2} + n_0^{5/2})(n_2^{5/2} + n_0^{5/2})} \tag{2.27}$$

The expression for ρ_{drag} is now in a form that leads to physical behavior, that qualitatively agrees with experiment, and is compatible with equation (2.23). As such, the next step is to substitute it into equation (2.23) which leads to a complicated expression given as

$$\begin{aligned}\overline{\rho}_{\text{drag}} = -C_0 \frac{n_1 n_2}{(n_1^{5/2} + n_0^{5/2})(n_2^{5/2} + n_0^{5/2})} - \frac{C_0}{2}(\delta {n_1}^2) \Bigg[\chi_{\text{sep}} \frac{(2n_0^{5/2} - 3n_1^{5/2})}{4(n_0^{5/2} + n_1^{5/2})^2} \frac{(2n_0^{5/2} - 3n_2^{5/2})}{(n_0^{5/2} + n_2^{5/2})^2} \\ + \frac{1}{2}\chi_{\text{sep}}^2 \Big(\frac{25n_2^4}{2(n_0^{5/2} + n_2^{5/2})^3} - \frac{35n_2^4}{4(n_0^{5/2} + n_2^{5/2})^2} \Big) \frac{n_1}{(n_1^{5/2} + n_0^{5/2})} \\ + \frac{1}{2} \Big(\frac{25n_1^4}{2(n_0^{5/2} + n_1^{5/2})^3} - \frac{35n_1^4}{4(n_0^{5/2} + n_1^{5/2})^2} \Big) \frac{n_2}{(n_2^{5/2} + n_0^{5/2})} \Bigg]\end{aligned} \tag{2.28}$$

where

$$C_0 = \frac{h\zeta(3)}{e^6 \cdot 1024} \frac{(k_{\text{B}}T)^2}{d^4} \tag{2.29}$$

Equation (2.28) serves as the main point of analysis for the rest of this work.

CHAPTER III

RESULTS AND FEATURE EXTRACTION

3.1 Contribution to $\overline{\rho}_{\text{drag}}$ when $n_2 = 0$;

In our model, there are only two sources that can contribute to $\overline{\rho}_{\text{drag}}$, one, of course being the electron density fluctuation, the other being the contribution coming from n_1 and n_2. To examine solely the contribution of electron density fluctuation to $\overline{\rho}_{\text{drag}}$, we set $n_2 = 0$ to eliminate any contribution n_2 might have back on $\overline{\rho}_{\text{drag}}$. Equation (2.28) then becomes

$$\overline{\rho}_{\text{drag}} = -\frac{C_0}{4}(\delta {n_1}^2)\chi_{\text{sep}}\frac{(2n_0^{5/2} - 3n_1^{5/2})}{n_0^{5/2}(n_0^{5/2} + n_1^{5/2})^2} \tag{3.1}$$

Figure 3.1 shows the behavior of equation 3.1 for a fixed χ_{sep}. The notable feature of equation (3.1), as seen in figure 3.1, is that as n_1 increases from zero, there exists a point where $\overline{\rho}_{\text{drag}}$ flips sign. This feature has been found in recent experiment and theory as discussed in the introduction, and serves as a primary feature of our model.

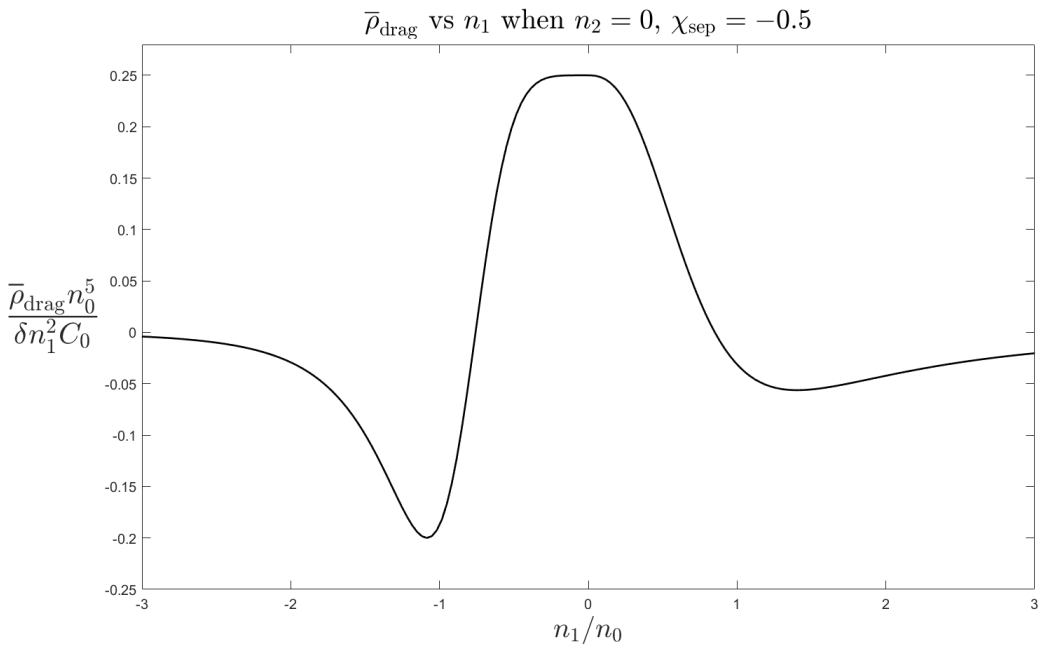

Figure 3.1: Behavior of equation (3.1) when χ_{sep} = -0.5 in reduced units. χ_{sep} was chosen arbitrarily between -1 and 0, as it is bound by these values and only acts as a scaling factor when $n_2 = 0$.

3.2 Symmetry of $\overline{\rho}_{\text{drag}}(n_1, n_2)$

In the following subsections, we will closely examine χ_{sep}, and its relation to any symmetry found between $\overline{\rho}_{\text{drag}}(n_1, n_2)$ and $\overline{\rho}_{\text{drag}}(n_2, n_1)$. We argue that this symmetry and χ_{sep} act as the links between how we qualitatively expect the system to behave, and how it quantitatively behaves. We notice that $-1 < \chi_{\text{sep}} < 0$ for constant intralayer distance d, through equation (2.22). It is easy to see that when $q \to 0$, $\chi_{\text{sep}} \to -1$, and when $q \to \infty$, $\chi_{\text{sep}} \to 0$. Thus, because $q > 0$, and because equation (2.22) is monotonic for $q > 0$, for all values of q with constant d, χ_{sep} is bound between -1 and 0.

3.2.1 Asymptotic regime when $\chi_{\text{sep}} \to 0$

Physically, the case when $\chi_{\text{sep}} \to 0$ corresponds to the asymptotic regime where the wave number of density fluctuation, q, is much larger than the inverse distance between the two sheets. For the $q \to \infty$ limit, the contribution of the oscillation in the first layer to the potential it creates will approach zero, as layer two will experience the first layer as being completely uniform so there will be no response from the density fluctuation in layer two. However the density fluctuation still contributes to $\overline{\rho}_{\text{drag}}$ through layer one. In the $\chi_{\text{sep}} \to 0$ limit, equation (2.28) becomes

$$\begin{aligned}\overline{\rho}_{\text{drag}} = -\frac{C_0}{4}(\delta {n_1}^2)\left[\left(\frac{25n_1^4}{2(n_0^{5/2}+n_1^{5/2})^3} - \frac{35n_1^{3/2}}{4(n_0^{5/2}+n_1^{5/2})^2}\right)\frac{n_2}{(n_2^{5/2}+n_0^{5/2})}\right] \\ -C_0\frac{n_1 n_2}{(n_1^{5/2}+n_0^{5/2})(n_2^{5/2}+n_0^{5/2})}\end{aligned} \tag{3.2}$$

Figures 3.2 and 3.3 show contour plots of $\overline{\rho}_{\text{drag}}$ as a function of n_1 and n_2 for various δn_1

Comparing equation (3.2) to (2.28), it is clear to see that this form (where $\chi_{\text{sep}} \approx 0$) minimizes symmetry between $\overline{\rho}_{\text{drag}}(n_1, n_2)$ and $\overline{\rho}_{\text{drag}}(n_2, n_1)$. A more comprehensive examination of this symmetry will be discussed in section 3.2.3.

3.2.2 Asymptotic regime when $\chi_{\text{sep}} \to -1$

The physical picture that this regime corresponds to is the case where, compared to a constant distance between plates d, the wavenumber of oscillation, q, is extremely small. This corresponds to the maximum response of the second layer to the oscillation in the first. As q becomes small, the wavelength of oscillation becomes very large, thus the difference between the peaks and valleys of the oscillation will be, on average, more easily felt by the second layer. In this case, if the layers suddenly reversed roles (the undriven layer becomes driven, and the driven layer becomes undriven), one should expect $\overline{\rho}_{\text{drag}}$ to stay the same. Quantitatively, it is expected that $\overline{\rho}_{\text{drag}}(n_1, n_2) = \overline{\rho}_{\text{drag}}(n_2, n_1)$. Under this regime, equation (2.28) becomes,

$$\begin{aligned}\overline{\rho}_{\text{drag}} = -C_0 \frac{n_1 n_2}{(n_1^{5/2} + n_0^{5/2})(n_2^{5/2} + n_0^{5/2})} + \frac{C_0}{2}(\delta {n_1}^2) \Bigg[& \frac{(2n_0^{5/2} - 3n_1^{5/2})}{4(n_0^{5/2} + n_1^{5/2})^2} \frac{(2n_0^{5/2} - 3n_2^{5/2})}{(n_0^{5/2} + n_2^{5/2})^2} \\ & - \frac{1}{2}\Big(\frac{25 n_2^4}{2(n_0^{5/2} + n_2^{5/2})^3} - \frac{35 n_2^{3/2}}{4(n_0^{5/2} + n_2^{5/2})^2} \Big) \frac{n_1}{(n_1^{5/2} + n_0^{5/2})} \\ & - \frac{1}{2}\Big(\frac{25 n_1^4}{2(n_0^{5/2} + n_1^{5/2})^3} - \frac{35 n_1^{3/2}}{4(n_0^{5/2} + n_1^{5/2})^2} \Big) \frac{n_2}{(n_2^{5/2} + n_0^{5/2})} \Bigg]\end{aligned} \tag{3.3}$$

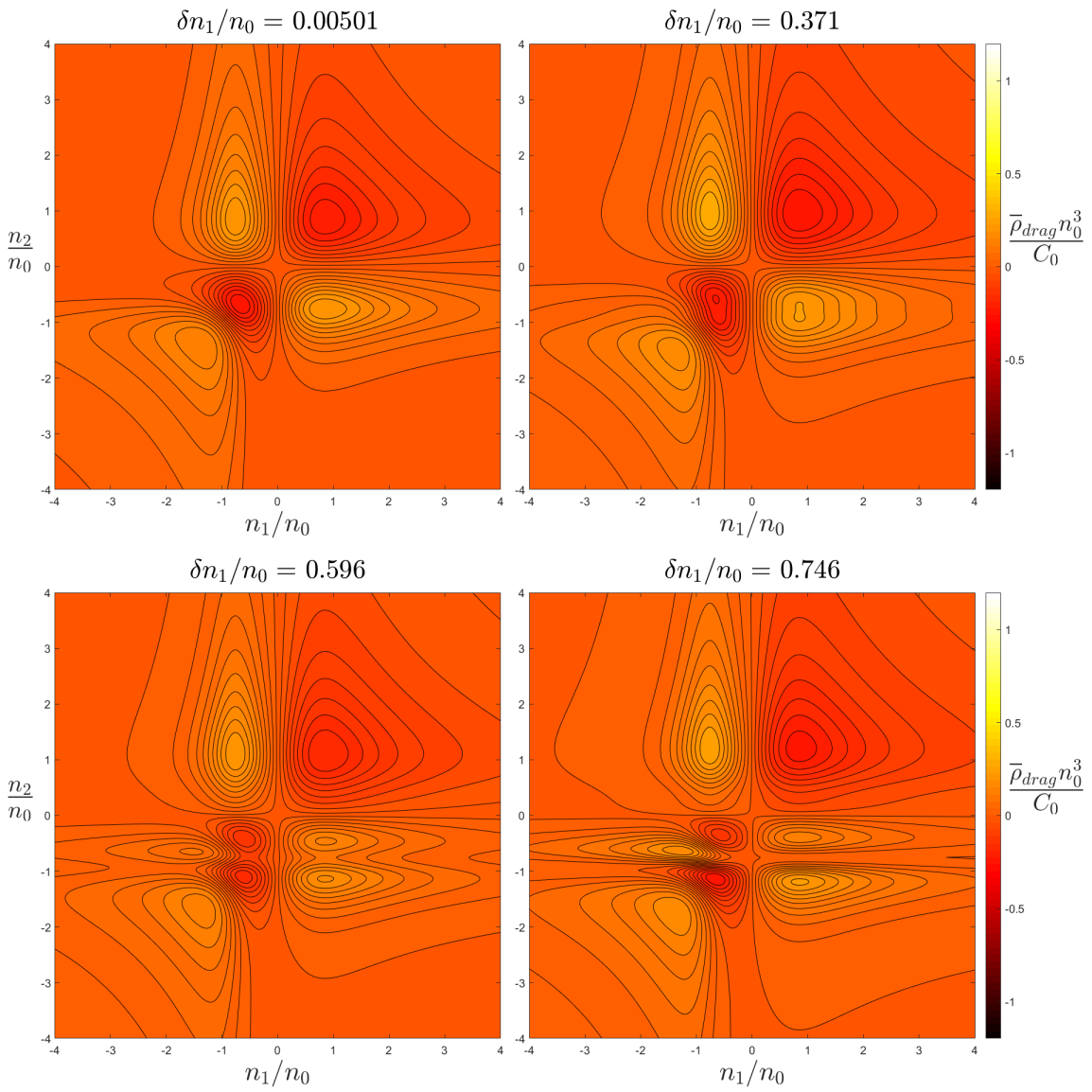

Figure 3.2: Contour plots of equation 3.2 for small δn_1 in the case when $\chi_{\text{sep}} = 0$. In reduced units, $\overline{\rho}_{drag}$ is shown as a function of n_2, n_1, and δn_1 whose value changes with each plot. Each δn_1 was chosen to highlight major qualitative behaviors between subplots. The colorbar scale does not change.

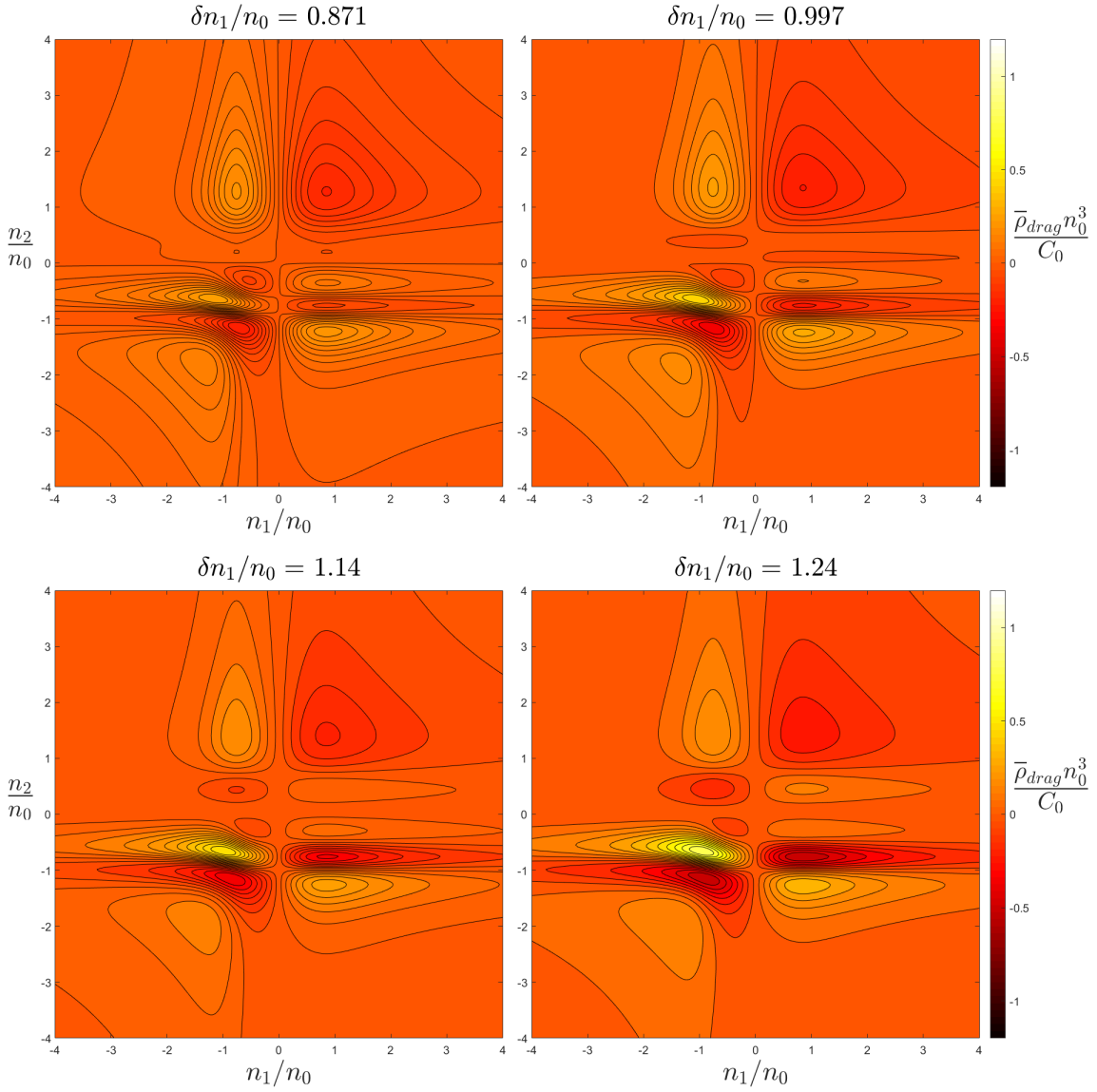

Figure 3.3: Contour plots of equation 3.2 for large δn_1in the case when $\chi_{\text{sep}} = 0$. In reduced units, $\overline{\rho}_{drag}$ is shown as a function of n_2, n_1, and δn_1 whose value changes with each plot. Each δn_1 was chosen to highlight major qualitative behaviors between subplots. The colorbar scale does not change.

It is easy to see the symmetry between n_1 and n_2 is verified in equation (3.8), as $\overline{\rho}_{\text{drag}}(n_1, n_2) = \overline{\rho}_{\text{drag}}(n_2, n_1)$. Figures 3.4 and 3.5 show this symmetry through contour plots, as in all δn_1 steps, n_1 and n_2 are symmetric about each other.

After the last subplot where $\delta n_1 = 1.22$ in figure 3.3, no further major qualitative changes occured within $\overline{\rho}_{\text{drag}}(n_1, n_2)$ with a further increasing δn_1. At this point, an increasing δn_1 only serves to further increase the peaks, and decrease the valleys found within figure 3.6, and as such we can estimate that this is the point where the second term in equation (3.3) begins to dominate the first.

3.2.3 Regime when $-1 < \chi_{\text{sep}} < 0$

In this regime, the degree by which $\overline{\rho}_{\text{drag}}(n_1, n_2)$ is symmetric to $\overline{\rho}_{\text{drag}}(n_2, n_1)$ is entirely dependent on how the term in equation (2.28) which includes χ^2_{sep} compares with the term immediately following it. To draw emphasis to these terms, we rewrite equation (2.28) as follows

$$\begin{aligned}\overline{\rho}_{\text{drag}} = ... + \frac{1}{2}\chi^2_{\text{sep}}\Big(\frac{25n_2^4}{2(n_0^{5/2}+n_2^{5/2})^3} - \frac{35n_2^{3/2}}{4(n_0^{5/2}+n_2^{5/2})^2}\Big)\frac{n_1}{(n_1^{5/2}+n_0^{5/2})} \\ + \frac{1}{2}\Big(\frac{25n_1^4}{2(n_0^{5/2}+n_1^{5/2})^3} - \frac{35n_1^{3/2}}{4(n_0^{5/2}+n_1^{5/2})^2}\Big)\frac{n_2}{(n_2^{5/2}+n_0^{5/2})}\Bigg]\end{aligned} \tag{3.4}$$

All other terms found within equation (2.28) are symmetric about n_1 and n_2, so they are ommitted from being considered. Assuming all other variables are constant, if $\chi_{\text{sep}} = -1$, then the two terms found in equation (3.4) are symmetric to each other. However, as χ_{sep} begins to increase towards zero, the contribution from the first term becomes increasingly *less* like the second term, thus breaking their symmetry. From

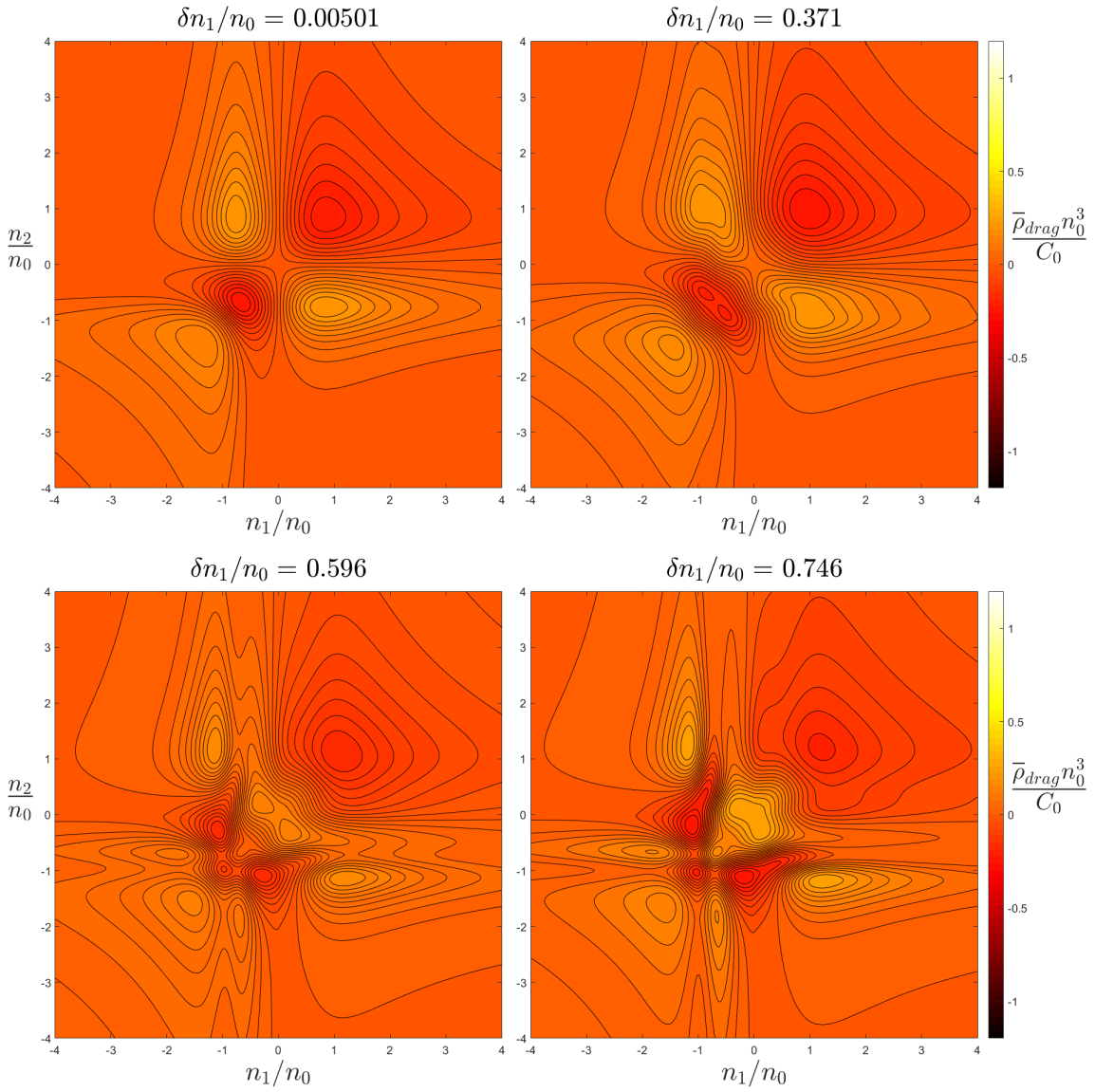

Figure 3.4: Contour plots of equation (3.3) for small δn_1in the case when $\chi_{\text{sep}} = -1$. In reduced units, $\overline{\rho}_{drag}$ is shown as a function of n_2, n_1, and δn_1 whose value changes with each plot. Each δn_1 was chosen to highlight major qualitative behaviors between subplots. The colorbar scale does not change.

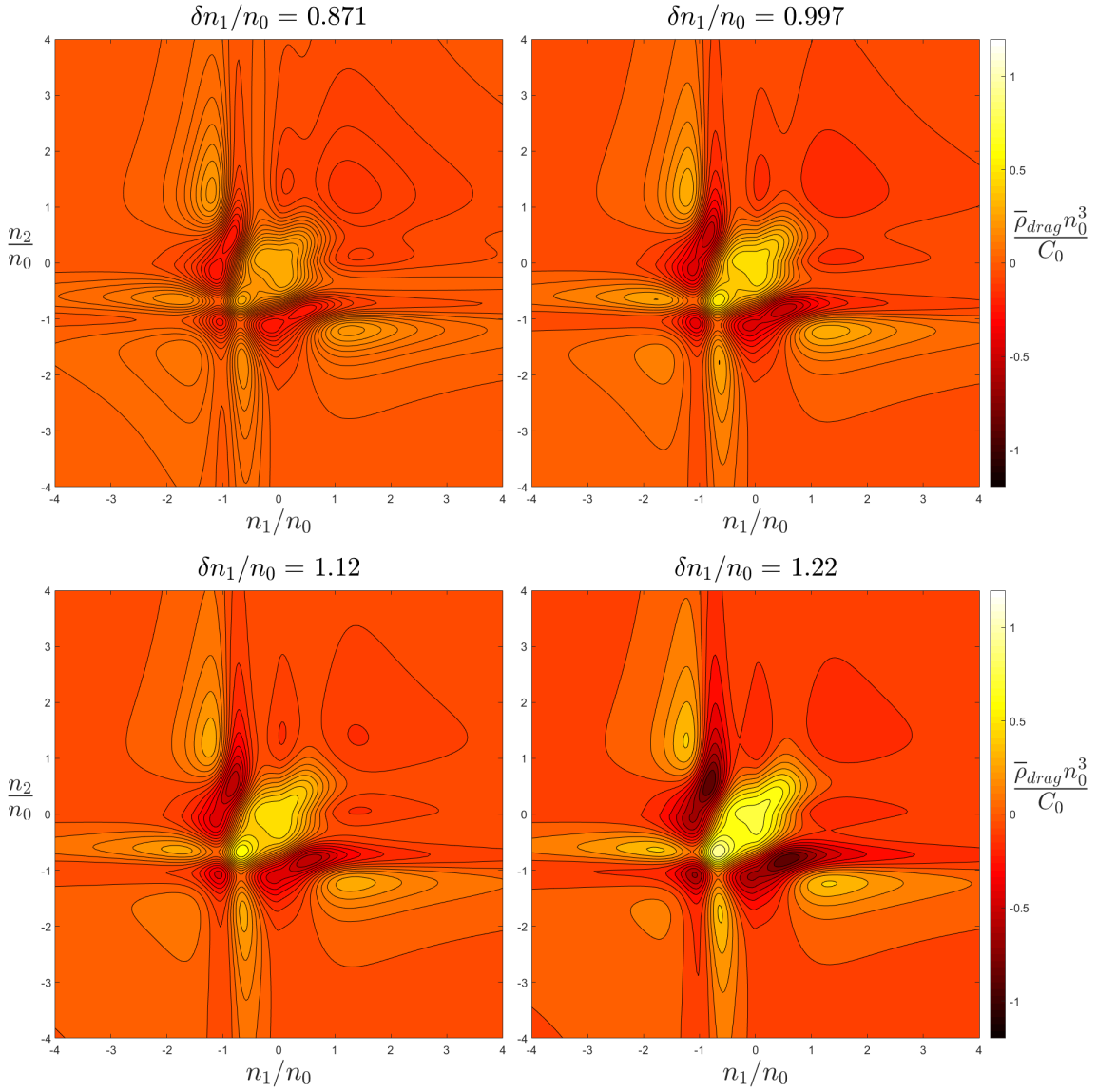

Figure 3.5: Contour plots of equation (3.3) for large δn_1in the case when $\chi_{\text{sep}} = -1$. In reduced units, $\overline{\rho}_{drag}$ is shown as a function of n_2, n_1, and δn_1 whose value changes with each plot. Each δn_1 was chosen to highlight major qualitative behaviors between subplots. The colorbar scale does not change.

this, we conclude that χ_{sep} acts as a measure of symmetry between $\overline{\rho}_{\text{drag}}(n_1, n_2)$ and $\overline{\rho}_{\text{drag}}(n_2, n_1)$ within our model, with symmetry being maximized at $\chi_{\text{sep}} = -1$, and symmetry being minimized at $\chi_{\text{sep}} = 0$.

3.3 Discussion

First and foremost, the results found above confirm our intuition about how $\overline{\rho}_{\text{drag}}$ should behave depending on the wave number of electron density fluctuation, q, and the distance between the two plates d. The relation between q and d is through χ_{sep}, which we have shown in section 3.2.3 is the measure of symmetry with respect to interchanging n_1 and n_2 within our model. Quantitatively, our model behaves exactly how we would qualitatively expect it to, with $\overline{\rho}_{\text{drag}}$ being symmetric around n_1 and n_2 when the frequency of electron density fluctuation, q, is very small compared to intralayer distance, d, and symmetry dissapearing when the frequency of electron density fluctuation is very large compared to the intralayer distance.

The main result in section 3.1, as n_1 increases from zero, with $n_2 = 0$ there exists an n_1 where $\overline{\rho}_{\text{drag}}$ changes sign, has been observed in both experiment and other theory. As such, our model is in agreement with this qualitative behavior.

CHAPTER IV

CONCLUSION

We have derived an expression for the drag transresistivity in a graphene double layer system exhibiting potential fluctuations modelled as a periodic oscillation in electron density. This simple model is the first attempt in the literature to shed light on the mechanisn by which correlations in electron density fluctuations in double layer graphene systems affect drag transresistivity. Our model starts from the Coulomb interaction and explicitely derives the correlation between n_2 and a sinusoidal fluctuation in n_1. The uniform case (no electron density fluctuation) emerges from our model as the amplitude of fluctuation approaches zero. When the amplitude of oscillation is non-zero, our model exhibits a change of sign in ρ_{drag} as n_1 increases from zero with $n_2 = 0$, which agrees with previous experiment[2, 3, 4] and theory results[5, 6]. Recent previous experiments have also shown a sudden sign change in ρ_{drag} as temperature is decreased [4]. The link between a changing temperature and a charge density oscillation both resulting in a sudden sign change in ρ_{drag} in unclear, and serves as an area of further research.

Omitted from this model is any consideration for any external magnetic or electric fields, which will be useful to consider for more complication systems of graphene sheets, such as a triple layer system, or a system where taking into account hall

drag is important. Further studies are also needed to more precisely determine how inhomogeneities within graphene vary in space.

BIBLIOGRAPHY

[1] B. N. Narozhny and A. Levchenko. Coulomb drag. *Rev. Mod. Phys.*, 88:025003, May 2016.

[2] J. I. A. Li, T. Taniguchi, K. Watanabe, J. Hone, A. Levchenko, and C. R. Dean. Negative coulomb drag in double bilayer graphene. *Phys. Rev. Lett.*, 117:046802, 2016.

[3] R.V. Gorbachev, A. K. Geim, M. I. Katsnelson, K. S. Novoselov, T. Tudorovskiy, I. V. Grigorieva, A. H. MacDonald, K. Watanabe, T. Taniguchi, and L. A. Ponomarkendo. Strong coulomb drag and broken symmetry in double-layer graphene. *Nature Phys*, 8:896–901, 2012.

[4] P Simonet, S Hennel, H Overweg, R Steinacher, M Eich, R Pisoni, Y Lee, P Märki, T Ihn, and K Ensslin. Anomalous coulomb drag between bilayer graphene and a gaas electron gas. *New Journal of Physics*, 19:103042, 2017.

[5] J. C. W. Song, D Abani, and L.S. Levitov. Coulomb drag mechanisms in graphene. *Nano Letters*, 13:3631–3637, 2013.

[6] Derek Ho, Indra Yudhistra, Ben Yu-Kuang Hu, and Adam Shaffique. Theory of coulomb drag in spatially inhomogeneous 2d materials. *Communications Physics*, 27:403–416, 2018.

[7] Wang-Kong Tse, Ben Yu-Kuang Hu, and S. Das Sarma. Theory of coulomb drag in graphene. *Phys. Rev. B*, 76:081401, 2007.

[8] M Carrega, T Tudorovskiy, A Principi, M.I. Katsnelson, and M Polini. Theory of coulomb drag for massless dirac fermions. *Journal of Computational Physics*, 124:93–114, 1996.

APPENDIX

POISSON'S EQUATION IN TWO DIMENSIONS

Poisson's Equation, written in notation consistent with chapter two, is as follows

$$-\bigtriangledown^2 \phi(\vec{r}) = \frac{\delta n(\vec{r})}{\varepsilon_0} \tag{A.1}$$

where δn is the charge density. The fourier transform in is then given as

$$Q^2\phi(\vec{Q}) = \frac{\delta\widetilde{n}(\vec{Q})}{\varepsilon_0} \tag{A.2}$$

Where $\vec{Q}$ is the 3-dimensional wave vector. We will rewrite $\vec{Q}$ as follows

$$\vec{Q} = \vec{q} + q_z\hat{z} \tag{A.3}$$

Where $\vec{q}$ lies in the $x-y$ plane. Our goal, however, is to find the relationship between ϕ and $\vec{q}$ for $z = 0$. To achieve this, we inverse Fourier transform in only the z direction.

$$\phi(\vec{q}, z) = \frac{1}{2\pi}\int_{-\infty}^{\infty}\phi(\vec{q}, q_z)e^{iq_z z}dq_z = \frac{1}{2\pi}\int_{-\infty}^{\infty}\frac{\delta\widetilde{n}(\vec{q})e^{iq_z z}}{\varepsilon_0(q^2+q_z^2)}dq_z = \frac{1}{2\pi}\frac{\delta\widetilde{n}(\vec{q})}{\varepsilon_0}\int_{-\infty}^{\infty}\frac{e^{iq_z z}dq_z}{q^2+q_z^2} \tag{A.4}$$

Through Euler's identity, the expression then becomes

$$\phi(\vec{q}, z) = \frac{1}{2\pi}\frac{\delta\widetilde{n}(\vec{q})}{\varepsilon_0}\int_{-\infty}^{\infty}\frac{(\cos(q_z z) + i\sin(q_z z))dq_z}{q^2+q_z^2} \tag{A.5}$$

The $\frac{i\sin(q_z z)}{q^2+q_z^2}$ term is odd, and as such once integrated will be zero. Therefore we will omit it from equation (A.5). This leads to

$$\phi(\vec{q},z) = \frac{1}{2\pi}\frac{\delta\widetilde{n}(\vec{q})}{\varepsilon_0}\int_{-\infty}^{\infty}\frac{\cos(q_z z)dq_z}{q^2+q_z^2} \tag{A.6}$$

The integral can be solved by contour integration and is given as

$$\int_{-\infty}^{\infty}\frac{\cos(q_z z)dq_z}{q^2+q_z^2} = \frac{\pi}{q}e^{-qz} \tag{A.7}$$

Using this result, equation (A.6) becomes

$$\phi(\vec{q},z) = \frac{\delta\widetilde{n}(\vec{q})}{2q\varepsilon_0}e^{-qz} \tag{A.8}$$

Equation (A.8) resembles equation (2.12) when $z = 0$.